JACS
JOURNAL OF THE AMERICAN CHEMICAL SOCIETY

pubs.acs.org/JACS

Article

Dialkyl Ether Formation at High-Valent Nickel

Franck Le Vaillant, Edward J. Reijerse, Markus Leutzsch, and Josep Cornella*

Cite This: https://dx.doi.org/10.1021/jacs.0c07381

Read Online

ACCESS | Metrics & More | Article Recommendations | Supporting Information

ABSTRACT: In this article, we investigated the I_2-promoted cyclic dialkyl ether formation from 6-membered oxanickelacycles originally reported by Hillhouse. A detailed mechanistic investigation based on spectroscopic and crystallographic analysis revealed that a putative reductive elimination to forge $C(sp^3)-OC(sp^3)$ using I_2 might not be operative. We isolated a paramagnetic bimetallic Ni^{III} intermediate featuring a unique $Ni_2(OR)_2$ (OR = alkoxide) diamond-like core complemented by a μ-iodo bridge between the two Ni centers, which remains stable at low temperatures, thus permitting its characterization by NMR, EPR, X-ray, and HRMS. At higher temperatures (>−10 °C), such bimetallic intermediate thermally decomposes to afford large amounts of elimination products together with iodoalkanols. Observation of the latter suggests that a $C(sp^3)-I$ bond reductive elimination occurs preferentially to any other challenging C−O bond reductive elimination. Formation of cyclized THF rings is then believed to occur through cyclization of an alcohol/alkoxide to the recently forged $C(sp^3)-I$ bond. The results of this article indicate that the use of F^+ oxidants permits the challenging $C(sp^3)-OC(sp^3)$ bond formation at a high-valent nickel center to proceed in good yields while minimizing deleterious elimination reactions. Preliminary investigations suggest the involvement of a high-valent bimetallic Ni^{III} intermediate which rapidly extrudes the C−O bond product at remarkably low temperatures. The new set of conditions permitted the elusive synthesis of diethyl ether through reductive elimination, a remarkable feature currently beyond the scope of Ni.

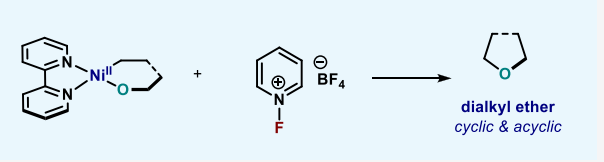

INTRODUCTION

Dialkyl ethers constitute one of the most valuable functional groups, and their synthesis represents one of the oldest strategies to build chemical complexity. As a result, formation of C−O bonds through the union of two organic fragments has prevailed one of the most powerful technologies, finding application across the chemical sciences: from covalent linkages and solid supports to crucial motifs in biologically active compounds.[1] From a synthetic point of view, formation of the C−O bond has largely relied on the venerable Williamson ether synthesis,[2] which involves the union of an alcohol and an alkyl halide through a S_N2 reaction in the presence of a strong base (Scheme 1A). The high practicality and scalability of this transformation has placed it as a cornerstone reaction in both academic and industrial settings.[3] Yet, the nucleophilic mechanism of the reaction is in turn its Achilles heel: the reaction efficiency is largely affected by the competitive alkoxide- or base-promoted E1 and E2 processes when secondary and tertiary alkyl halides are utilized. To circumvent these limitations, organic chemists have devoted their efforts in developing many strategies to produce highly coveted ethers—electrochemistry,[4] organocatalysis,[5] Lewis acid/base catalysis,[6] among others. Nevertheless, one of the most promising alternatives in the literature to forge C−O bonds relies on the mediation of transition metals. Exploiting their redox properties, transition metal catalysis has been demonstrated to be one of the pillars in the construction of these linkages.[7] For example, Chan-Lam or Ullmann couplings

Scheme 1. (A) Williamson Ether Synthesis (Advantages and Pitfalls); (B) Existing Methods for $C(sp^2)-O$ Bond Formation Using Ni Catalysts; (C) $C(sp^3)-O-C(sp^3)$ Bond Formation from High-Valent Ni

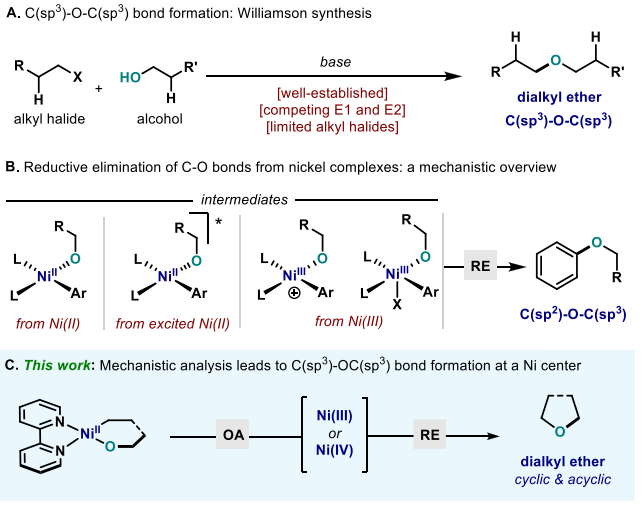

Received: July 14, 2020

have experienced great success and found broad application for the synthesis of a myriad of highly relevant ethers.[8] Despite the advantages associated with these methods, they have been largely dominated by linkages such as $C(sp^2)-O-C(sp^2)$ and $C(sp^2)-O-C(sp^3)$. In addition, Pd catalysis has also experienced tremendous development in this front, providing catalytic methods for $C(sp^2)-O$ bond formation.[9−11] Yet, Pd complexes that permit construction of dialkylethers ($C(sp^3)-O-C(sp^3)$) through reductive elimination still present severe challenges.[12] A remarkable example of the formation of cyclic ethers is the Co-catalyzed radical cyclization of alkenols from Mukaiyama,[13] which has found ample success in various synthetic endeavors.[13c]

Other first-row transition metals (Cu, Fe, Ni)[14,15] have also been demonstrated to excel as catalysts in various C−O coupling strategies.[16] In particular, Ni-catalyzed transformations have gained tremendous momentum for their enormous capabilities in forging C−heteroatom bonds.[17] A seminal work by Hartwig described the possibility to forge $C(sp^2)-O-C(sp^3)$ bonds using $Ni(COD)_2$ and dppf as the optimal catalytic system.[18] Encompassing Hartwig's precedent, Stradiotto described a general $C(sp^2)-O$ bond formation from L_2Ni^{II} complexes capitalizing on a newly designed set of phosphine-based ligands (L = CyPAd-DalPhos)[19] (Scheme 1B). More recently, methods that replace the phosphine by simple diamine ligands have been reported, which rely on access to high-valent[20] or high-energy[21] Ni complexes through light irradiation, which rapidly forge the $C(sp^2)-O$ bond. Mechanistic investigations on these latter approaches revealed that $C(sp^2)-O$ bond formation can proceed either via a Ni^{III} intermediate or via an excited Ni^{II} complex after energy transfer (Scheme 1B).[22] In 2020, Ackermann and co-workers developed a nickel-catalyzed electrochemical $C(sp^2)-H$ alkoxylation, which proceeds through a Ni^{III} intermediate.[23] Recently, Nocera reported a Ni^{I}-catalyzed etherification protocol that mimics the reactivity of photoredox-catalyzed couplings without the use of a light source or photocatalyst.[24] Similarly to the metallaphotoredox protocols, it is believed that the high oxidation state of the Ni^{III} intermediate provides the necessary driving force to undergo $C(sp^2)-O$ bond linkage upon reductive elimination. Whereas realization of $C(sp^2)-O-C(sp^3)$ through reductive elimination at a Ni center is well precedented and studied,[25] a fundamental mechanistic understanding of the analogous process to forge dialkyl ethers through $C(sp^3)-OC(sp^3)$ reductive elimination still remains elusive with virtually no systematic studies on their feasibility (Scheme 1C).[26]

In the 1990s, Hillhouse provided one of the first examples of $C(sp^3)-O-C(sp^3)$ bond formation from well-defined oxanickelacycles (**1a−e**) bearing bipyridine ligands and using stoichiometric I_2 as oxidant (Scheme 2A).[27] In these seminal reports, involvement of high-valent nickel species such as $Ni^{III}-I$ or $Ni^{IV}-I$ complexes was suggested; yet, minimal evidence was provided, and such intermediates remained purely speculative. Interestingly, when I_2 was replaced by other oxidants such as O_2 or ferrocenium (Fc^+) the $C(sp^3)-OC(sp^3)$ bond formation was not observed.[27d] In addition, higher yields were obtained for those complexes where β-hydride elimination is hampered by the limited conformations of the oxanickelacycles (Scheme 2A). As a result, formation of the $C(sp^3)-OC(sp^3)$ bond was limited to cyclic products, as exemplified by the incapacity of **1f** to deliver the corresponding acyclic dialkyl ether.[27b] On the basis of these early results, Love

Scheme 2. I_2-Promoted $C(sp^3)-O-C(sp^3)$ Bond Formation: (A) Hillhouse's Seminal Work with Bipyridine Oxanickelacycles; (B) Love's Example Using Strained Oxanickelacycle with Bidentate Phosphine

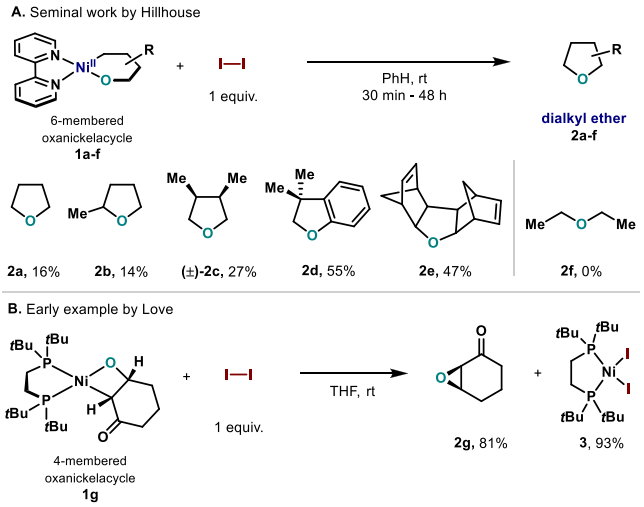

and co-workers capitalized on the I_2-promoted C−O bond formation and applied it to the oxanickelacyclobutane **1g** bearing a 1,2-bis(di-*tert*-butylphosphino)ethane (dtbpe) as the ligand (Scheme 2B).[28] The authors observed rapid and clean formation of the corresponding epoxide in good yield along with almost quantitative formation of the corresponding $(dtbpe)NiI_2$ (**3**). In this case, deleterious β-hydride elimination is not operative due to the presence of a ketone. To the best of our knowledge, these reports represent solitary examples present in the literature regarding formation of dialkyl ethers from well-defined organometallic species. Despite the powerful reactivity observed, no evidence of the intermediates involved has been reported. Yet, fundamental understanding of the key parameters that govern this particular transformation would provide tremendous insights for the design of future catalytic $C(sp^3)-O-C(sp^3)$ ether syntheses. Herein, we report a comprehensive mechanistic study on the transformation originally described by Hillhouse: characterization of the reaction intermediates revealed formation of a robust and paramagnetic Ni^{III} dimer, which thermally decomposes to afford primarily elimination products. Additional mechanistic data suggests that direct $C(sp^3)-OC(sp^3)$ reductive elimination from such Ni^{III} intermediate to forge simple THF rings is highly unlikely. On the contrary, experimental evidence supports an alternative mechanism based on a preferential $C(sp^3)-I$ reductive elimination followed by an intramolecular S_N2 reaction. Yet, all of these drawbacks were overridden by the replacement of I_2 by fluorine-containing oxidants which prevent not only competitive C−X reductive elimination but also deleterious elimination side reactions. In this manner, high yields of the cyclized tetrahydrofurans were obtained.

RESULTS AND DISCUSSION

Initially, we considered that oxanickelacyles **1a** and **1b** provided an excellent platform to investigate an oxidative $C(sp^3)-OC(sp^3)$ bond formation (Scheme 3). Both complexes represent challenging substrates to undergo intramolecular C−O bond formation (Scheme 2A) due to the dynamic behavior of the alkoxide anion as a result of the fluxionality of the alkyl backbone. Subsequently, diverse

https://dx.doi.org/10.1021/jacs.0c07381
J. Am. Chem. Soc. XXXX, XXX, XXX−XXX

Scheme 3. Synthetic Route to Oxanickelacyclohexanes[31]

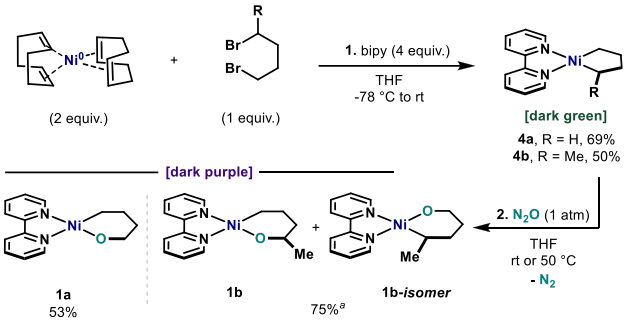

[a]This yield comprises a mixture of 85:15 of **1b** and **1b-*isomer***.

conformations of the CH and CH_2 groups can be adopted which could lead to unproductive β-hydride elimination or simple E2. With these potential drawbacks in mind, we set out to synthesize nickelacyclopentanes **4a** and **4b** as described in the literature:[27,29] the corresponding 1,4-alkyldibromides (1.0 equiv) were reacted with an excess of $Ni(COD)_2$ (2.0 equiv) and bipyridine (bipy, 4.0 equiv) at −78 °C in THF. After warming up to 25 °C, the mixture is filtered and the dark-green complexes **4a** and **4b** are obtained in 69% and 50% yield, respectively (step 1, Scheme 3). Subsequently, **4a** and **4b** were subjected to O-atom insertion using N_2O following Hillhouse's procedure.[27] After exposing **4a** and **4b** to N_2O atmosphere (1 atm) in THF, oxanickelacyclohexane complexes **1a** and **1b** were obtained as deep purple solids in 53% and 75% yield, respectively (step 2, Scheme 3). It is important to mention that to access high-purity **1a** and **1b**, further filtration is required through Avicel[30] in order to remove some colloidal nickel particles.[31] Complexes **1a** and **1b** exhibit remarkable stability in the solid state and can be stored in the freezer of the glovebox. Yet, solutions of **1a** and **1b** slowly degrade, probably through decoordination of the alkoxide ligand, which complicates purification. Indeed, purities that ranged from 85% to 93% could be achieved for **1a** and **1b** after a series of crystallizations and filtrations. Such Ni^{II} complexes are square planar and easily characterized by NMR in the diamagnetic region.[31] Whereas **1a** offers inherent symmetry, **1b** is not symmetric and different products can arise in the O-atom insertion step (step 2, Scheme 3). Compound **1b** has both a 1° and 2° carbons, and the selectivity for the O insertion was found to be 85:15, favoring isomer **1b** over **1b-*isomer***.[32] However, considering that the reductive elimination of both isomers would lead to the same THF product **2b**, no further separation was attempted. For clarity, only structure **1b** will be used in the following schemes.

With these complexes in hand, cyclic voltammetry studies were performed in order to gain insight into their redox properties. As shown in Figure 1, the cyclic voltammogram of complex **1b** in CD_3CN revealed two oxidative waves at −0.70 and +0.31 V against Fc/Fc^+. Interestingly, the first oxidative wave is not reversible, whereas the second wave is quasi-reversible. On the basis of other similar CVs for well-defined cyclic $(bipy)Ni^{II}(alkyl)(aryl)$ and $(terpy)Ni^{II}(C_4F_8)$ complexes,[33] we tentatively assigned the redox potentials to the corresponding single-electron oxidation Ni^{II}/Ni^{III} and Ni^{III}/Ni^{IV} couples, respectively. It is worth pointing out that the low values for both processes manifest the facility of **1b** to access high-valent Ni intermediates.[34]

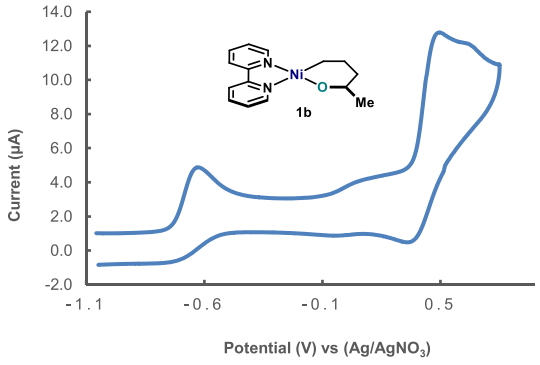

Figure 1. Cyclic voltammogram of **1b** (1.0 mM) in CD_3CN, recorded versus $Ag/AgNO_3$ electrode, using n-Bu_4NPF_6 (0.2 M) as electrolyte, under argon, with a scan rate of 100 $mV{\cdot}s^{-1}$. Potentials are then converted to the Fc/Fc^+ couple.[31]

On the basis of the oxidation potential obtained for **1b** ($E_{1/2}(Ni^{II}/Ni^{III})$ = −0.70 V, $E_{1/2}(Ni^{III}/Ni^{IV})$ = +0.31 V vs Fc/Fc^+ in CD_3CN), it is reasonable to propose that oxidation of this complex to the corresponding Ni^{III} should be feasible using Fc^+ or O_2.[27d] However, Hillhouse already noticed that Fc^+ and O_2 did not lead to any C−O bond formation in good yield. Indeed, when **1b** was oxidized with $FcBF_4$, mainly the elimination product was obtained (**6b**) with only trace amounts of $C(sp^3)-OC(sp^3)$ bond formation (Scheme 4).

Scheme 4. Attempts to C−O Bond Formation after One-Electron Oxidation of 1b To Access High-Valent Ni^{III}

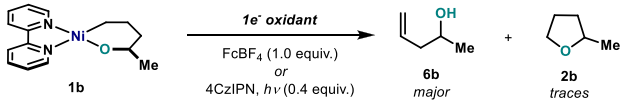

Other single-electron oxidants were tested, such as photocatalyst 4CzIPN (2,4,5,6-tetra(9*H*-carbazol-9-yl)-isophthalonitrile (**5**),[35] which would also lead to cationic Ni^{III} intermediates. Yet, no desired THF ring **2b** could be detected in the crude mixture. These results suggest that a $C(sp^3)-OC(sp^3)$ reductive elimination from cationic Ni^{III} intermediates is unlikely (vide infra).

To gain further insight into the C−O bond-forming event, the reaction reported by Hillhouse and co-workers was repeated: complex **1b** (1.0 equiv) was reacted with I_2 (1.1 equiv) in CD_2Cl_2 at 25 °C.[36] To our surprise, upon addition of I_2 to a solution of **1b**, the color of the reaction mixture quickly changed from deep purple to orange. After 20 min of stirring at 25 °C, brown solids precipitated from the solution. At this point, the solids were filtered off and the filtrate was analyzed by ^1H NMR and GC-MS. Surprisingly, the desired cyclic ether **2b** was not observed (Scheme 5A). On the other hand, significant amounts of pent-4-en-2-ol (**6b**, 45%) were obtained, presumably through side-elimination reactions. More importantly, peaks relative to 5-iodopentan-2-ol (**7b**, 10%) were detected and successfully assigned.[31] The presence of **7b** was further confirmed by GC-MS. After solubilizing the solids, analysis by ^1H NMR revealed a set of broad paramagnetic peaks, suggesting the presence of ligated bipy−Ni species. HRMS analysis of the solid indicated that a possible structure could be $(bipy)NiI_2$,[28] although dimeric compounds could not be ruled out.[37] Slow crystallization in CD_2Cl_2 at −20 °C led to crystals suitable for X-ray analysis, which unequivocally

https://dx.doi.org/10.1021/jacs.0c07381
J. Am. Chem. Soc. XXXX, XXX, XXX−XXX

Scheme 5. (A) Hillhouse I_2-Promoted C(sp^3)−O−C(sp^3) Bond Formation Reaction (Analysis of the Fate of the Organic and Inorganic Compounds); (B) X-ray Structure of Complex 8;[31a] (C) Ni^{III} Bimetallic Intermediate 9a−b; (D) ^1H NMR of Paramagnetic Complex 9a[31b]

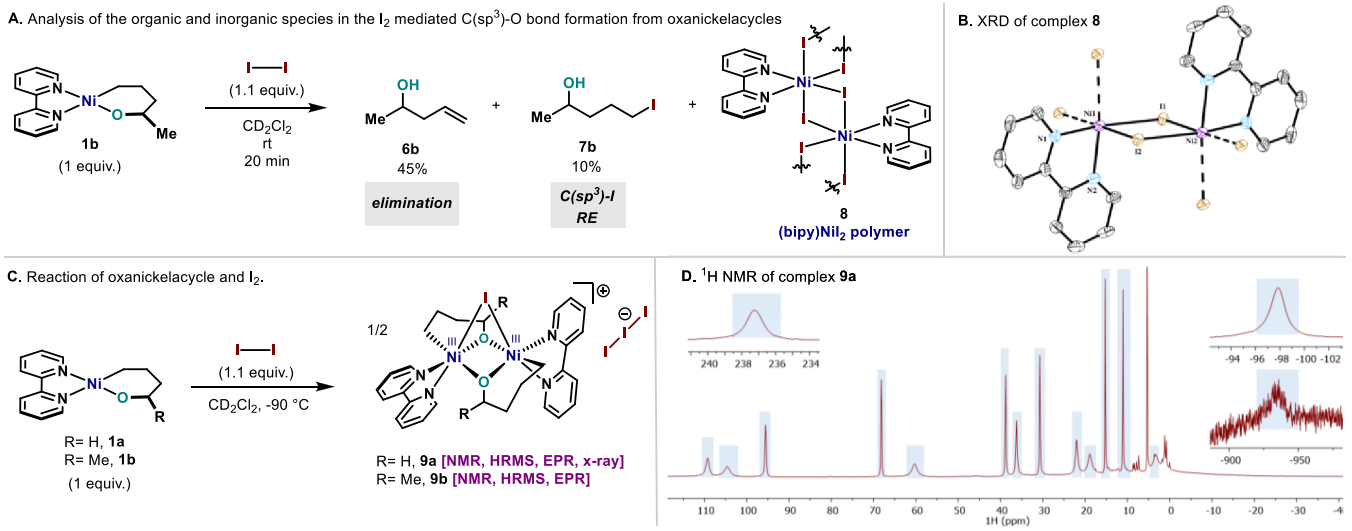

[a]Disordered iodine atoms are omitted for clarity. Selected distances (Angstroms): Ni1−I1 = N2−I2 = 2.78; Ni1−I2 = Ni2−I1 = 2.83; Ni1−N1 = Ni1−N2 = 2.07. Selected angles (degrees): I1−Ni−I2 = 89.2; Ni1−I1−Ni2 = 94.2. [b]Insets correspond to peaks at 237, −98, and −930 ppm.

confirmed formation of a polymeric (bipy)NiI_2 (**8**) consisting of octahedral Ni complexes linked together by μ-iodo bridges (Scheme 5B).

Considering the redox potential of iodine ($E_{1/2}(I_2/I_2^{-\bullet})$ = +0.21 V vs Fc^+/Fc),[38] it is reasonable to assume formation of a high-valent nickel Ni^{III}−I complex upon mixing **1a** and **1b** with I_2. However, similarly to the case of Fc^+, formation of Ni^{IV} is highly unlikely. To investigate whether Ni^{III}−I intermediates are formed in the reaction system, we decided to monitor the reaction by ^1H NMR at low temperature. Upon adding a cold solution of I_2 (1.1 equiv) to a solution of **1a** in a J-Young tube at −90 °C, a rapid color change was observed from deep purple to deep orange (Scheme 5C). Complete conversion of **1a** to a new set of well-defined signals was observed. The ^1H NMR spectrum at −90 °C exhibits peaks ranging from −930 to +237 ppm, pointing to a paramagnetic complex (Scheme 5D).[31] Upon storing a concentrated solution at −35 °C, good-quality crystals formed. X-ray analysis unambiguously determined that the intermediate consisted of a symmetric cationic Ni^{III} bimetallic complex (**9a**). This complex represents a unique and unprecedented structure of a dinuclear Ni^{III} with several structural and electronic interesting features (Figure 2). First, **9a** contains two Ni^{III} atoms in an octahedral arrangement with a large Ni−Ni distance of 2.84 Å, thus suggesting no metal−metal interaction.[39] In addition, **9a** features a rather unique μ-iodo bridge unifying both Ni atoms with a highly strained Ni1−I1−Ni2 angle of 58.07°. As a result, the I is bridging both Ni^{III} centers through an elongated Ni−I bond (Ni1−I1 = Ni2−I1, 2.92 Å). It is important to mention that Ni^{III} dimers with one bridging halogen atom have been recently proposed as intermediates in C(sp^2)−X (X = Br, Cl, I) bond formation.[39a,40] However, the most striking feature of **9a** is the diamond-like core formed by the Ni atoms and the alkoxide ligands. Two μ_2-bridging alkoxide anions join the two Ni centers in a highly symmetric environment (Ni1−O1 = Ni1−O2 = Ni2−O1 = Ni2−O2, 2.00 Å) with angles of Ni1−O1−Ni2 = 92.72° and O1−Ni1−O2 = 79.57°. The Ni−O distances for **9a** are in the range of other bis(μ_2-oxide)-bridging Ni^{III} complexes known in the literature.[41] The complex is complemented by the bipyridine ligands with similar Ni−N distances for both N (Ni1−N1, 1.99 Å; Ni1−N2, 2.05 Å). Finally, the remaining position of the octahedron is occupied by the alkyl residue with Ni−C(sp^3) distances resembling those reported for other Ni^{III}−C(sp^3) bonds (Ni1−C1, 2.013 Å).[42] A parallel behavior was observed when complex **1b** was reacted with I_2. However, attempts to obtain crystals of the Ni^{III} intermediate were unsuccessful. Bimetallic complexes **9a** and **9b** were further characterized by HRMS both in ESI^+ and in ESI^- modes.[31] Finally, due to the paramagnetic nature of complexes **9a** and **9b**, further structural and electronic characterization was attempted by electron paramagnetic resonance (EPR).

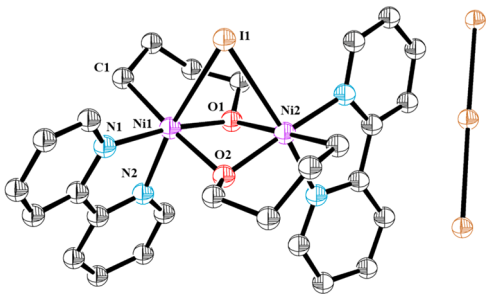

Figure 2. X-ray structure of compound **9a**.[31] Hydrogen atoms and disordered iodide atoms in I_3^- counterion are omitted for clarity. Selected distances (Angstroms): Ni1−Ni2 = 2.84; Ni1−I1 = Ni2−I1 = 2.92; Ni1−O1 = Ni1−O2 = Ni2−O1 = Ni2−O2 = 2.00; Ni1−N1 = 1.99; Ni1−N2 = 2.05; Ni1−C1 = 2.013. Selected angles (degrees): Ni1−I1−Ni2 = 58.07; Ni1−O1−Ni2 = 92.72; O1−Ni1−O2 = 79.57.

The EPR spectra of complexes **9a** and **9b** were recorded at the X-band, 30 K, and are depicted in Figure 3. As expected, the EPR spectra of **9a** and **9b** are very similar but show subtle differences in line splitting and intensity ratio between the different spectral features. The multiple line splitting suggests an electron−electron spin−spin interaction between the two Ni^{III} centers. This means that the dimer structure found in the

https://dx.doi.org/10.1021/jacs.0c07381
J. Am. Chem. Soc. XXXX, XXX, XXX−XXX

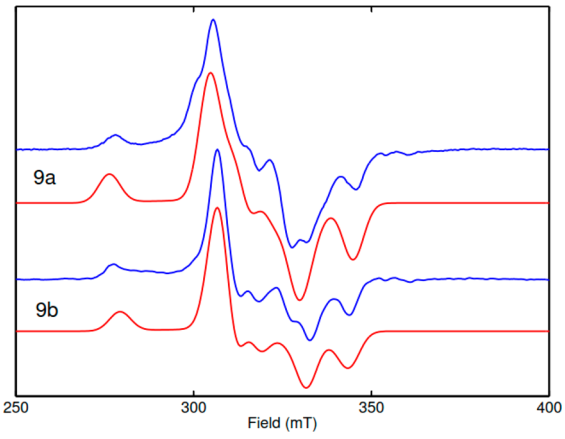

Figure 3. X-band EPR (9.623 GHz) of complexes **9a** and **9b** recorded at 30 K (blue traces).[31] Experimental parameters: 1 mW, 100 kHz, 7.5 G field modulation. Red traces represent the Easyspin[43] (esfit) simulation with the following parameters: g(**9a**) = (2.081, 2.155, 2.279); g(**9b**) = (2.084, 2.144, 2.287). Dipolar interaction D(**9b**) = 517 MHz; D(**9a**) = 550 MHz. J coupling < 50 MHz.

solid state (Figure 2) is retained in solution for both complexes. Making use of the symmetry properties of the dimer complex,[31] we were able to simulate the EPR spectra as shown in Figure 3. The g-matrix principal values obtained for **9a** (2.081, 2.155, 2.279) and **9b** (2.084, 2.144, 2.287) are similar to what has been observed for a similar *N,N*-ligand-coordinated Ni^{III} monomer complex (2.03, 2.14, 2.20).[40] The magnetic interaction between the two Ni^{III} centers is dominated by the dipolar contribution found to be (0.9, 1.1, −2)*550 MHz for **9a** and (0.9, 1.1, −2)*517 MHz for **9b**. The J coupling between the two Ni^{III} centers is very small (50 MHz), and its effect on the EPR is only visible as a small splitting at the center of the spectrum. As confirmed by DFT analysis,[31] the two Ni^{III} centers effectively behave as isolated S = 1/2 systems. This is in agreement with NMR analysis, estimating the magnetic susceptibility of the dimer complex using the Evans method to be S = 1/2 for each Ni^{III} center.[31]

Having identified and characterized **9**, we set out to explore its reactivity. Upon slowly warming solutions of **9a** and **9b** in CD_2Cl_2 from −90 to 25 °C, several interesting observations were made. First, the chemical shifts of complexes **9a** and **9b** are highly dependent on the temperature, which further confirms the paramagnetic nature of **9**.[31] Moreover, **9a** and **9b** have a remarkable stability across a wide range of temperatures, from −90 to −10 °C. Beyond −10 °C, rapid evolution of **9a** and **9b** to terminal alkenes **6a** and **6b** and iodoalcohols **7a** and **7b** is observed. While traces of THF could be detected in the case of **9a**, no detectable amount of the $C(sp^3)$−$OC(sp^3)$ bond formation product **2b** was observed for **9b**.[44] This last observation indicates that the $C(sp^3)$−I reductive elimination is kinetically more favorable to any other C−O bond-forming event at Ni. Whereas such $C(sp^3)$−I bond formation proceeds via a reductive elimination from Ni^{III}−I or direct attack of the I counterion to the Ni−$C(sp^3)$ bond in a S_N2 fashion is currently unknown.[42,45] However, a similar system was recently reported by Diao, suggesting that $C(sp^3)$−I bond formation could proceed through monomeric square pyramid Ni^{III} complexes.[40] Hence, it is plausible to think that after dissociation of **9a** and **9b**, a similar process could be operative.

The absence of **2b** upon warming **9b** to 25 °C together with rapid consumption of oxanickelacycle **1b** at −90 °C toward preferential formation of **6b** and **7b** led us to consider that the $C(sp^3)$−$OC(sp^3)$ bond formation pathway accounting for the ca. 10−14% yield of **2b** may arise from a slow intramolecular cyclization of the iodoalkoxide/iodoalcohol in a S_N2 fashion.[46] Indeed, after 48 h of reaction time in the NMR tube without stirring, the iodoalcohol formed initially slowly evolves to form **2b** (Scheme 6).[31] It is well established that 5-iodoalkoxides can

Scheme 6. Thermal Decomposition of Complex 9b and Hypothetical S_N2 Reaction from 7b

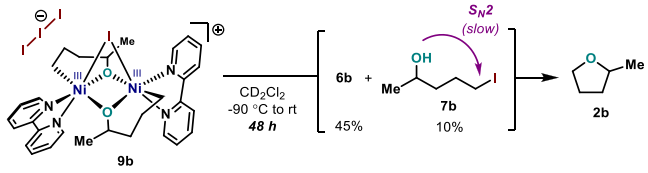

undergo intramolecular 5-*exo-tet* cyclization to afford cyclic ethers.[47] This experimental evidence supports the lack of reactivity when attempting formation of open-chain ethers such as Et_2O (**2f**) due to the much slower rates for intermolecular S_N2 reactions.[48]

With these results in hand, we addressed such a defying and elusive reductive elimination. It was clear that other oxidants that enable access to high-valent Ni species should be scrutinized.[49] When I_2 was replaced by Umemoto's reagent (*S*-(trifluoromethyl)dibenzothiophenium triflate, TDTT, **10a**),[33a] a low yield of **2b** was observed (10%). A reduced amount of side product **6b** was obtained when CD_3CN was used instead. During monitoring studies at variable temperatures, HCF_3 (boiling point = −82.1 °C) was detected. Formation of fluoroform suggests the involvement of CF_3−Ni−H intermediates and points to alkenol **6b** being formed through β-hydride elimination pathways. In addition to alkenol **6b** and HCF_3, other byproducts containing $C(sp^3)$−CF_3 were also identified by ^{19}F NMR, which was consistent with formation of high-valent Ni intermediates.[50] Despite the low yields, to the best of our knowledge, this challenging $C(sp^3)$−CF_3 bond formation is unprecedented at a Ni center.[51] At this point, it was quite evident that competitive $C(sp^3)$−X reductive eliminations (X = I, CF_3) should be suppressed if the challenging $C(sp^3)$−O−$C(sp^3)$ is to be achieved. Hence, we speculated that the presence of F ligands in the coordination sphere of a high-valent Ni intermediate would dramatically reduce the observed side reactions due to the high kinetic barrier to forge $C(sp^3)$−F bonds.[52] When **1b** was mixed with 1.05 equiv of XeF_2 in CD_2Cl_2 or CD_3CN, immediate reaction took place and the desired ether **2b** was observed as the major product in 60% or 47% yield, respectively.[50a,52f,53] Interestingly, formation of **6b** remained minor in CD_2Cl_2 and could be largely suppressed in CD_3CN (8%). It is important to mention that products derived from a putative $C(sp^3)$−F reductive elimination were only observed in trace amounts.[31] In this line, when XeF_2 was replaced by SelectFluor (**10c**) in CD_3CN a similar outcome was obtained with a 45% yield of **2b** along with a minimal amount of **6b** (10%). We then investigated several commercially available substituted 1-fluoro-pyridinium salts (**10d**−**f**) as they have increased solubility in CH_3CN.[54] Using **10d**, 45% **2b** and <5% **6b** were obtained. Gratifyingly, when using NFTPB (**10e**, *N*-fluoro-2,4,6-trimethylpyridinium tetrafluoroborate) and NFTPT (**10f**, *N*-fluoro-2,4,6-trimethylpyridinium triflate) an

https://dx.doi.org/10.1021/jacs.0c07381
J. Am. Chem. Soc. XXXX, XXX, XXX−XXX

increase in the yield of **2b** was observed (61% and 63%, respectively). Notice that when using BF_4 as counterion, formation of **6b** could be minimized to a residual 8%. As expected, **2a** was also obtained in a satisfactory 56% and 63% yield when using **10e** and **10f**, respectively (Scheme 7B).

Scheme 7. (A) Screening of Oxidants for the Oxidatively Induced C(sp³)–OC(sp³) Bond Formation;[a] (B) Application to the Synthesis of THF

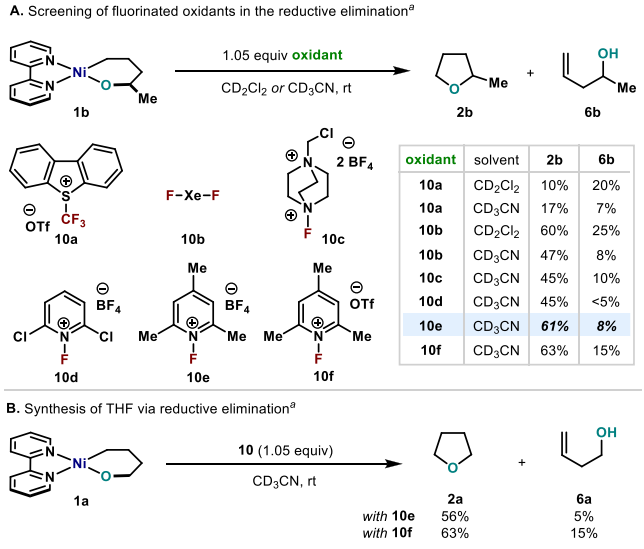

oxidant	solvent	2b	6b
10a	CD_2Cl_2	10%	20%
10a	CD_3CN	17%	7%
10b	CD_2Cl_2	60%	25%
10b	CD_3CN	47%	8%
10c	CD_3CN	45%	10%
10d	CD_3CN	45%	<5%
10e	CD_3CN	*61%*	*8%*
10f	CD_3CN	63%	15%

[a]Reaction conditions: oxanickelacycle **1b** (1 equiv), oxidant **10** (1.05 equiv) in CD_3CN or CD_2Cl_2 at 25 °C.

Having identified a set of conditions that enable formation of cyclic C(sp³)–O–C(sp³) bonds at high-valent Ni centers, we speculated that a similar pathway should be valid for formation of acyclic ethers. In order to study this possibility, an acyclic precursor was synthesized through a two-step sequence (Scheme 8A). Following the protocol from Ikeda,[55] we initially synthesized (bipy)$NiEt_2$ (**11**) by reacting bipy, $Ni(acac)_2$, and $(EtO)AlEt_2$ in Et_2O for 50 h at 25 °C. After isolation via filtration (87%), the deep green solid **11** is subjected to N_2O atmosphere at 25 °C, allowing smooth O insertion into the Ni–C(sp³) bond,[27a,b] leading to (bipy)Ni(Et)(OEt) (**1f**) in 63% yield. At this point, **1f** was subjected to our optimized oxidation conditions using **10f** in CD_3CN at 25 °C (Scheme 8B). Gratifyingly, rapid formation of Et_2O (**2f**) was observed in 20% yield at 25 °C. A similar result was obtained using **10e**. Formation of **2f** from **1f** represents a unique example of C(sp³)–OC(sp³) bond formation and contrasts with the results obtained from Hillhouse, where C(sp³)–OC(sp³) bond formation from acyclic Ni^{II} complexes could not be achieved (see Scheme 2A). This unprecedented result for unbiased, acyclic substrates combined with the use of simple pyridinium salt **10e** and **10f** as a mild oxidant provides an interesting proof-of-concept for the development of new strategies based on Ni and may open the door to new avenues for catalytic dialkyl ether syntheses in the future.

Scheme 8. (A) Synthesis of (bipy)$NiEt_2$ 11 and (bipy)Ni(Et)(OEt) 1f;[a] (B) Oxidatively Induced Synthesis of Diethyl Ether from Nickel Complex 1f[b]

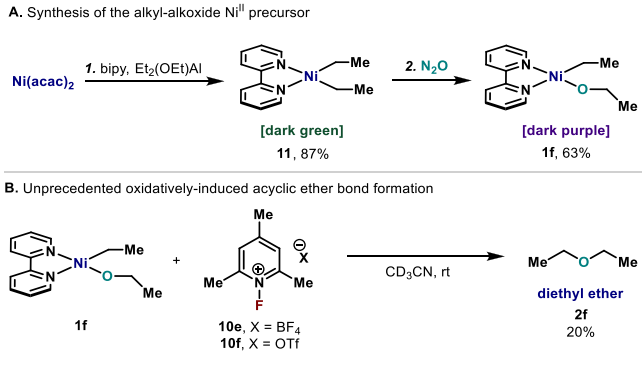

[a]Reaction conditions: (step 1) $Ni(acac)_2$ (1 equiv), bipy (1 equiv) Et_2AlOEt (3 equiv) in Et_2O, from −50 to 25 °C, 50 h, **11** 87% isolated yield; (step 2) **11** (1 equiv), N_2O (1 atm) in THF at 25 °C, **1f** 63% isolated yield. [b]Reaction conditions: oxanickelacycle **1f** (1 equiv), **10e** and **10f** (1.05 equiv) in CD_3CN at 25 °C, 1 min. Yields determined by ^1H NMR using mesitylene as internal standard.

Successful formation of C(sp³)–O–C(sp³) bonds using *N*-fluoropyridinium reagents posed the question of what is the exact nature of the high-valent Ni species involved in the process. On the basis of the CV results for **2b** (Figure 1) together with the oxidation results using Fc^+, O_2, and 4CzIPN photocatalyst (Scheme 4),[27] it is evident that access to Ni^{III} species is facile;[49] yet, cationic Ni^{III} are not capable of C–O bond formation due to fast elimination side reactions. It is important to point out that owing to the extremely fast reaction rates for C–O bond formation, mechanistic investigations on this particular system pose an experimental challenge. Indeed, **1a**, **1b**, **10e**, and **10f** react at −90 °C in <1 min, and no Ni intermediates could be detected spectroscopically (^1H and ^{19}F NMR). Attempts to stabilize high-valent Ni species using tripodal ligands (tris(pyrazolyl)borate[56] or tris(pyridyl)methane)[33a,49] resulted in degradation or failed to incorporate O to the Ni^{II}–C(sp³) bond. To our delight however, a signal could be detected by EPR from reaction of **1b** with **10f**. Such species were very short lived, but a sufficient amount could be trapped after rapid (1 s) mixing at −95 °C (melting point of PhMe) and subsequent freezing in liquid N_2 (Scheme 9A). The EPR spectrum showed multiple splitting features consistent with a Ni^{III} dimer species (***int-I***, Scheme 9B). The width of the spectrum, however, is reduced with respect to that of **9a** and **9b**, suggesting a reduction in the dipolar interaction between the two Ni^{III} centers. Indeed, spectral fits resulted in a smaller value (299 vs 517 and 550 MHz), whereas the *g*-tensor only differed slightly.[31] It is important to point out that although the fitting parameters for ***int-I*** are probably not unique due to the few spectral features and large number of free parameters, the current fits would be consistent with a Ni^{III} dimer with symmetry properties resembling **9a**.[57] Additional information about the putative intermediates was provided by mass spectrometry analysis. When a low-temperature mixture of **1b** and **10f** was analyzed by mass spectrometry, a *m*/*z* corresponding to ***int-I*** could be detected. In addition, *m*/*z* consistent with structures such as ***int-II*** (or **1b**) and ***int-IV*** were also identified.[58] Although the nature of the exact species prior to reductive elimination still remains elusive, several possibilities are envisaged. On one hand, dissociation of ***int-I*** would afford ***int-II*** and ***int-III*** (path a).[59] An alternative pathway would involve a disproportionation of ***int-I*** into starting oxanickelacycle **1b** and ***int-IV*** (path c).[60] Reductive elimination could then occur from either ***int-III*** or ***int-IV***. The high degree of elimination obtained in Scheme 4 when using Fc^+ or 4CzIPN would argue against path

https://dx.doi.org/10.1021/jacs.0c07381
J. Am. Chem. Soc. XXXX, XXX, XXX–XXX

Scheme 9. (A) EPR of *int-I* at 20 K;[a] (B) Mass Spectrometry Results and Postulated Mechanistic Pathways

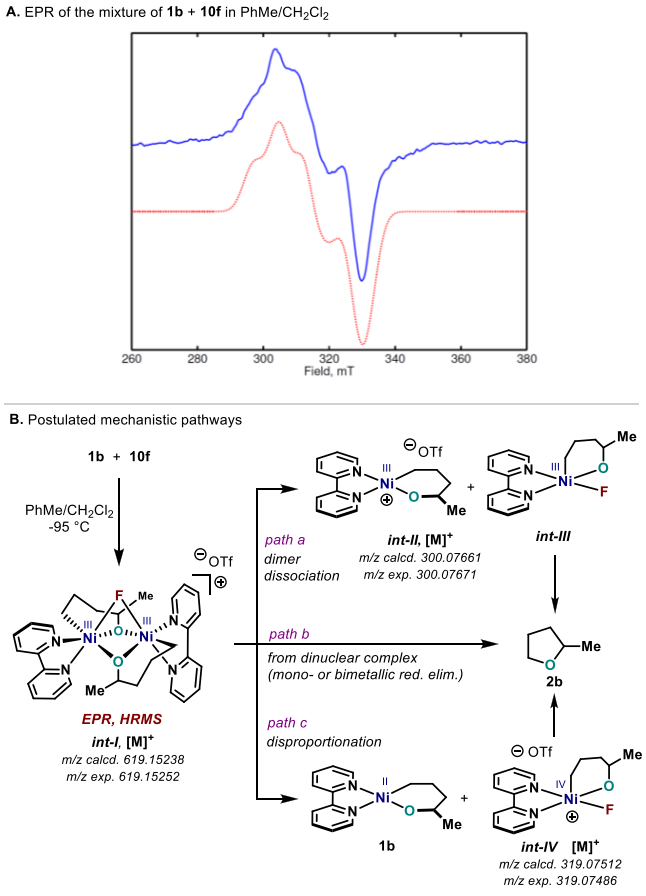

[a]Experimental conditions: Power = 2.0 mW, modulation (100 kHz) amplitude 7.5 G. Dotted red trace represents the Easyspin[43] (esfit) simulation with parameters g = (2.103, 2.200, 2.227). Dipolar interaction D(***int-I***) = 299 MHz. J coupling = 100 MHz.

a as a major contributor. Moreover, another possible pathway could involve direct reductive elimination from the dinuclear complex ***int-I*** (path b), which has been postulated for certain C−heteroatom and C−C bond-forming events.[40,61] In an attempt to discern between mechanistic pathways, we carried out the oxidation of **1b** with only 0.5 equiv of **10f**. In this case, one-half of the yield of **2b** observed in Scheme 7A was obtained (35−40%) without trace amounts of **6b**.[31] The absence of elimination byproducts suggests that cationic Ni^{III} species might not be present and adds additional evidence about path a not being operative. However, the variety of pathways by which the C−O bond could be formed manifests the need for further mechanistic investigations to fully elucidate the nature of the intermediates involved.

CONCLUSIONS

In conclusion, we studied the seminal I_2-promoted C−O bond formation reported by Hillhouse toward formation of cyclic ethers (**2a** and **2b**). A detailed mechanistic investigation revealed formation of **9a** and **9b**, an unprecedented Ni^{III} bimetallic structure as a cationic intermediate, which was fully characterized by NMR, EPR, HRMS, and X-ray in the case of **9a**. These paramagnetic complexes feature a unique $Ni_2(OR)_2$ (OR = alkoxide) diamond-like core complemented by a μ-iodo bridge between the two Ni centers. The anionic counterion of the complexes consists of the linear I_3^-, which remains in the outer sphere of the robust bimetallic cation. Thermal decomposition of **9** beyond −10 °C leads primarily to elimination products (**6**). In addition, substantial amounts of iodoalkanols (**7**) were detected through preferential C(sp^3)−I reductive elimination. The low yields obtained for **2a** and **2b** are postulated to arise from an intramolecular S_N2 reaction from **7** over long periods of time. This manifests that the original mechanistic picture for direct C(sp^3)−OC(sp^3) bond formation through reductive elimination is extremely challenging for simple THF rings. Cyclic voltammetry studies as well as a survey of oxidants identified the use of fluoropyridinium reagents **10e** and **10f** as excellent candidates to afford good yields of **2** while minimizing formation of elimination byproducts (**6**). In addition, this new set of conditions was successfully applied in the elusive synthesis of acyclic diethyl ether (**2f**) from a well-defined Ni^{II} complex. Preliminary mechanistic studies revealed that upon oxidation of **1** with **10**, a highly reactive intermediate could be detected in solution by EPR and HRMS, which is consistent with a Ni^{III} dimeric structure (***int-I***). Efforts to fully characterize the high-valent species involved after oxidation and prior to reductive elimination are currently under investigation in our laboratory. We believe the findings reported here open the door to new avenues for Ni catalysis and could aid practitioners in the field to unravel novel metal-catalyzed ether synthesis.

ASSOCIATED CONTENT

Supporting Information

The Supporting Information is available free of charge at https://pubs.acs.org/doi/10.1021/jacs.0c07381.

Experimental procedures and analytical data (^{1}H, ^{19}F, and ^{13}C NMR, EPR, X-ray, HRMS, CV) (PDF)

CIF file for compound **8**, also available free of charge from the www.ccdc.cam.ac.uk under CCDC number 2014828 (CIF)

CIF file for compound **9a**, also available free of charge from the www.ccdc.cam.ac.uk under CCDC number 2014830 (CIF)

CIF file for compound **S1**, also available free of charge from the www.ccdc.cam.ac.uk under CCDC number 2014829 (CIF)

AUTHOR INFORMATION

Corresponding Author

Josep Cornella − *Max-Planck-Institut für Kohlenforschung, Mülheim an der Ruhr 45470, Germany;* orcid.org/0000-0003-4152-7098; Email: cornella@kofo.mpg.de

Authors

Franck Le Vaillant − *Max-Planck-Institut für Kohlenforschung, Mülheim an der Ruhr 45470, Germany;* orcid.org/0000-0002-2723-1787

Edward J. Reijerse − *Max-Planck-Institut für Chemische Energiekonversion, Mülheim an der Ruhr 45470, Germany;* orcid.org/0000-0001-9605-4510

Markus Leutzsch − *Max-Planck-Institut für Kohlenforschung, Mülheim an der Ruhr 45470, Germany;* orcid.org/0000-0001-8171-9399

Complete contact information is available at: https://pubs.acs.org/10.1021/jacs.0c07381

https://dx.doi.org/10.1021/jacs.0c07381
J. Am. Chem. Soc. XXXX, XXX, XXX−XXX

Notes

The authors declare no competing financial interest.

■ ACKNOWLEDGMENTS

Financial support for this work was provided by the Max-Planck-Gesellschaft, Max-Planck-Institut für Kohlenforschung, and Fonds der Chemischen Industrie (VCI-FCI). F.L.V. thanks the Swiss National Science Foundation for an Early Mobility Postdoctoral Fellowship (Grant no. 184406). Sigrid Lutz is acknowledged for help in the synthesis of (bipy)$Ni(Et)_2$. We thank M. Kochius for technical support with low-temperature NMR measurements. The analytical departments (X-ray crystallography, NMR spectroscopy, and Mass spectrometry) at the MPI für Kohlenforschung are gratefully acknowledged for support in characterization of the compounds. We thank Prof. Dr. T. Ritter for providing access to the photoredox equipment in his laboratory. E.J.R. thanks Frank Reikowski and Dr. Leonid Rapatskiy for technical assistance with the EPR measurements. We thank Petra Hoefer and Dr. Christophe Werlé from the Max-Planck-Institut für Chemische Energiekonversion (MPI-CEC) for assistance in the cyclic voltammetry studies. We are thankful to Prof. Dr. A. Fürstner for insightful discussions and generous support.

■ REFERENCES

(1) (a) Roughley, S. D.; Jordan, A. M. The medicinal chemist's toolbox: an analysis of reactions used in the pursuit of drug candidates. *J. Med. Chem.* **2011**, *54*, 3451. (b) Brown, A.; Brown, L.; Brown, T. B.; Calabrese, A.; Ellis, D.; Puhalo, N.; Smith, C. R.; Wallace, O.; Watson, L. Triazole oxytocin antagonists: identification of aryl ether replacements for a biaryl substituent. *Bioorg. Med. Chem. Lett.* **2008**, *18*, 5242. (c) Backes, B. J.; Ellman, J. A. Solid support linker strategies. *Curr. Opin. Chem. Biol.* **1997**, *1*, 86. (d) Ganesan, A Wang resin. *Encyclopedia of reagents for organic synthesis*; Wiley: Hoboken, NJ, 2003. (e) Harris, J. M. *Poly(ethylene glycol) Chemistry: Biotechnical and Biomedical Applications*; Plenum Press: New York, 1992.

(2) Williamson, A. W. J. *Chem. Soc.* **1852**, *4*, 229. Alexander William Williamson (1824−1904) discovered this reaction in 1850 at University College, London

(3) For selected reviews on Williamson ether synthesis, see: (a) Li, J. J. Williamson ether synthesis. *Name Reactions*; Springer:Cham, 2014. (b) Wang, Z. Williamson Ether Synthesis. *Comprehensive Organic Name Reactions and Reagents*; John Wiley & Sons: Hoboken, NJ, 2010; pp 3026−3030.

(4) Xiang, J.; Shang, M.; Kawamata, Y.; Lundberg, H.; Reisberg, S.; Chen, M.; Mykhailiuk, P.; Beutner, G.; Collins, M.; Davies, A.; Del Bel, M.; Gallego, G.; Spangler, J.; Starr, J. T.; Yang, S.; Blackmond, D.; Baran, P. S. Hindered Dialkyl Ether Synthesis via Electrogenerated Carbocations. *Nature* **2019**, *573*, 398.

(5) Shibutani, S.; Kodo, T.; Takeda, M.; Nagao, K.; Tokunaga, N.; Sasaki, Y.; Ohmiya, H. Organophotoredox-Catalyzed Decarboxylative $C(sp^3)$−O Bond Formation. *J. Am. Chem. Soc.* **2020**, *142*, 1211.

(6) (a) Ghosh, A. K.; Tomaine, A. J.; Cantwell, K. E. Lewis Acid Mediated Cyclizations: Diastereoselective Synthesis of Six- to Eight-Membered Substituted Cyclic Ethers. *Synthesis* **2017**, *49*, 4229. (b) Trost, B. M.; Mata, G. Enantioselective Palladium-Catalyzed [3 + 2] Cycloaddition of Trimethylenemethane and Fluorinated Ketones. *Angew. Chem., Int. Ed.* **2018**, *57*, 12333. (c) De Nanteuil, F.; Serrano, E.; Perrotta, D.; Waser, J. Dynamic Kinetic Asymmetric [3 + 2] Annulation Reactions of Aminocyclopropanes. *J. Am. Chem. Soc.* **2014**, *136*, 6239. (d) Parsons, A. T. M.; Johnson, J. S. Catalytic Enantioselective Synthesis of Tetrahydrofurans: A Dynamic Kinetic Asymmetric [3 + 2] Cycloaddition of Racemic Cyclopropanes and Aldehydes. *J. Am. Chem. Soc.* **2009**, *131*, 3122. (e) Tsuji, N.; Kennemur, J. L.; Buyck, T.; Lee, S.; Prevost, S.; Kaib, P. S. J.; Bykov, D.; Fares, C.; List, B. Activation of olefins via asymmetric Brønsted acid catalysis. *Science* **2018**, *359*, 1501. (f) Luo, C.; Bandar, J. S. Superbase-Catalyzed anti-Markovnikov Alcohol Addition Reactions. *J. Am. Chem. Soc.* **2018**, *140*, 3547. (g) Shigeno, M.; Hayashi, K.; Nozawa-Kumada, K.; Kondo, Y. Phosphazene Base *t*Bu-P4 Catalyzed Methoxy−Alkoxy Exchange Reaction on (Hetero)Arenes to Aryl Alkenes. *Chem. - Eur. J.* **2019**, *25*, 6077.

(7) (a) Vedernikov, A. N. C−O Reductive Elimination from High Valent Pt and Pd Centers. In *C-X Bond Formation. Topics in Organometallic Chemistry*; Vigalok, A., Ed.; Springer, Berlin, Heidelberg, 2010; Vol. *31*. (b) Stambuli, J. P. New Trends in Cross-Coupling: Theory and Application. In *Transition Metal-Catalyzed Formation of C−O and C−S Bonds*; Colacot, T. J., Eds.; Royal Society of Chemistry: Cambridge, UK, 2014; Vol. *254*.

(8) (a) Munir, I.; Zahoor, A. F.; Rasool, N.; Naqvi, S. A. R.; Zia, K. M.; Ahmad, R. Synthetic applications and methodology development of Chan−Lam coupling: a review. *Mol. Diversity* **2019**, *23*, 215. (b) Qiao, J. X.; Lam, P. Y. S. In *Boronic Acids:Preparation and Applications in Organic Synthesis, Medicine and Materials*; Hall, D. G., Ed.; Wiley-VCH: Weinheim, 2011; pp 315−361. (c) Sambiagio, C.; Marsden, S. P.; Blacker, A. J.; McGowan, P. C. Copper catalysed Ullmann type chemistry: from mechanistic aspects to modern development. *Chem. Soc. Rev.* **2014**, *43*, 3525. (d) Monnier, F.; Taillefer, M. Catalytic C−C, C−N, and C−O Ullmann-Type Coupling Reactions. *Angew. Chem., Int. Ed.* **2009**, *48*, 6954.

(9) For seminal Pd-catalyzed $C(sp^2)$−O bond formation, see: (a) Mann, G.; Hartwig, J. F. Palladium Alkoxides: Potential Intermediacy in Catalytic Amination, Reductive Elimination of Ethers, and Catalytic Etheration. Comments on Alcohol Elimination from Ir(III). *J. Am. Chem. Soc.* **1996**, *118*, 13109. (b) Palucki, M.; Wolfe, J. P.; Buchwald, S. L. Palladium-Catalyzed Intermolecular Carbon-Oxygen Bond Formation: A New Synthesis of Aryl Ethers. *J. Am. Chem. Soc.* **1997**, *119*, 3395. (c) Torraca, K. E.; Huang, X.; Parrish, C. A.; Buchwald, S. L. An Efficient Intermolecular Palladium-Catalyzed Synthesis of Aryl Ethers. *J. Am. Chem. Soc.* **2001**, *123*, 10770.

(10) For recent works on Pd-catalyzed $C(sp^2)$−O bond formation, see: (a) Mikus, M. S.; Sanchez, C.; Fridrich, C.; Larrow, J. F. Palladium Catalyzed C−O Coupling of Amino Alcohols for the Synthesis of Aryl Ethers. *Adv. Synth. Catal.* **2020**, *362*, 430. (b) Zhang, H.; Ruiz-Castillo, P.; Schuppe, A. W.; Buchwald, S. L. Improved Process for the Palladium-Catalyzed C−O Cross-Coupling of Secondary Alcohols. *Org. Lett.* **2020**, *22*, 5369. (c) Zhang, H.; Ruiz-Castillo, P.; Buchwald, S. L. Palladium-Catalyzed C−O Cross-Coupling of Primary Alcohols. *Org. Lett.* **2018**, *20*, 1580. (d) Gowrisankar, S.; Sergeev, A. G.; Anbarasan, P.; Spannenberg, A.; Neumann, H.; Beller, M. A General and Efficient Catalyst for Palladium-Catalyzed C−O Coupling Reactions of Aryl Halides with Primary Alcohols. *J. Am. Chem. Soc.* **2010**, *132*, 11592. (e) Maligres, P. E.; Li, J.; Krska, S. W.; Schreier, J. D.; Raheem, I. T. C−O Cross-Coupling of Activated Aryl and Heteroaryl Halides with Aliphatic Alcohols. *Angew. Chem., Int. Ed.* **2012**, *51*, 9071. (f) Sawatzky, R. S.; Hargreaves, B. K. V.; Stradiotto, M. A Comparative Ancillary Ligand Survey in Palladium-Catalyzed C−O Cross-Coupling of Primary and Secondary Aliphatic Alcohols. *Eur. J. Org. Chem.* **2016**, *2016*, 2444.

(11) (a) Canty, A. J.; Jin, H.; Skelton, B. W.; White, A. H. Oxidation of Complexes by $(O_2CPh)_2$ and $(ER)_2$ (E = S, Se), Including Structures of $Pd(CH_2CH_2CH_2CH_2)(SePh)_2(bpy)$ (bpy = 2,2′-Bipyridine) and $MMe_2(SePh)_2(L_2)$ (M = Pd, Pt; L_2 = bpy, 1,10-Phenanthroline) and C−O and C−E Bond Formation at Palladium(IV). *Inorg. Chem.* **1998**, *37*, 3975. (b) Dick, A. R.; Hull, K. L.; Sanford, M. S. A Highly Selective Catalytic Method for the Oxidative Functionalization of C−H Bonds. *J. Am. Chem. Soc.* **2004**, *126*, 2300. (c) Desai, L. V.; Hull, K. L.; Sanford, M. S. Palladium-Catalyzed Oxygenation of Unactivated sp^3 C−H Bonds. *J. Am. Chem. Soc.* **2004**, *126*, 9542. (d) Giri, R.; Liang, J.; Lei, J.-G.; Li, J.-J.; Wang, D.-H.; Chen, X.; Naggar, I. C.; Guo, C.; Foxman, B. M.; Yu, J.-Q. Pd-Catalyzed Stereoselective Oxidation of Methyl Groups by Inexpensive Oxidants under Mild Conditions: A Dual Role for Carboxylic

https://dx.doi.org/10.1021/jacs.0c07381
J. Am. Chem. Soc. XXXX, XXX, XXX−XXX

Anhydrides in Catalytic C−H Bond Oxidation. *Angew. Chem., Int. Ed.* **2005**, *44*, 7420. (e) Canty, A. J.; Ariafard, A.; Camasso, N. M.; Higgs, A. T.; Yates, B. F.; Sanford, M. S. Computational study of $C(sp^3)$−O bond formation at a Pd^{IV} centre. *Dalton Trans.* **2017**, *46*, 3742. (f) Zhuang, Z.; Yu, J.-Q. Lactonization as a General Route to β-$C(sp^3)$−H Functionalization. *Nature* **2020**, *577*, 656. (g) Zhuang, Z.; Herron, A. N.; Fan, Z.; Yu, J.-Q. Ligand-Enabled mono-Selective β-$C(sp^3)$−H Acyloxylation of Free Carboxylic Acids Using a Practical Oxidant. *J. Am. Chem. Soc.* **2020**, *142*, 6769. (h) Whitehurst, W. G.; Gaunt, M. J. Synthesis and Reactivity of Stable Alkyl-Pd(IV) Complexes Relevant to Monodentate N-Directed $C(sp^3)$−H Functionalization Processes. *J. Am. Chem. Soc.* **2020**, *142*, 14169.

(12) Recent examples of Pd-catalyzed alkoxylations suggested the intermediacy of Pd^{IV} complexes prior to the reductive elimination, see: (a) Zhang, S.-Y.; He, G.; Zhao, Y.; Wright, K.; Nack, W. A.; Chen, G. Efficient Alkyl Ether Synthesis via Palladium-Catalyzed, Picolinamide Directed Alkoxylation of Unactivated $C(sp^3)$−H and $C(sp^2)$−H Bonds at Remote Positions. *J. Am. Chem. Soc.* **2012**, *134*, 7313. (b) Chen, Y.-Q.; Wu, Y.; Wang, Z.; Qiao, J. X.; Yu, J.-Q. Transient Directing Group Enabled Pd-catalyzed gamma-$C(sp^3)$−H Oxygenation of Alkyl Amines. *ACS Catal.* **2020**, *10*, 5657.

(13) (a) Inoki, S.; Mukaiyama, T. A Convenient Method for the Stereoselective Preparation of *trans*-2-Hydroxymethyltetrahydrofurans by the Oxidative Cyclization of 5-Hydroxy-1-alkenes with Molecular Oxygen Catalyzed by Cobalt(II) Complex. *Chem. Lett.* **1990**, *19*, 67. (b) Morra, B.; Morra, N. A.; MacDonald, D. G.; Pagenkopf, B. L. Gram-Scale Synthesis of the $Co(nmp)_2$ Catalyst to Prepare *trans*-2,5-Disubstituted Tetrahydrofurans by the Aerobic Oxidative Cyclization of Pent-4-en-1-ols. *Synthesis* **2020**, *52*, 847. (c) Heinrich, M.; Murphy, J. J.; Ilg, M. K.; Letort, A.; Flasz, J. T.; Philipps, P.; Fürstner, A. Chagosensine: A Riddle Wrapped in a Mystery Inside an Enigma. *J. Am. Chem. Soc.* **2020**, *142*, 6409.

(14) For recent work on Cu catalyzed $C(sp^3)$−O bond formation, see: (a) Hu, H.; Chen, S.-J.; Mandal, M.; Pratik, S. M.; Buss, J. A.; Krska, S. W.; Cramer, C. J.; Stahl, S. S. Copper-Catalysed Benzylic C−H Coupling with Alcohols via Radical Relay Enabled by Redox Buffering. *Nature Catal.* **2020**, *3*, 358. (b) Cheng, Y. F.; Liu, J.-R.; Gu, Q.-S.; Yu, S.-L.; Wang, J.; Li, Z.-L.; Bian, J.-Q.; Wen, W.-T.; Wang, X.-J.; Hong, X.; Liu, X.-Y. Catalytic Enantioselective Desymmetrizing Functionalization of Alkyl Radicals via Cu(I)/CPA Cooperative Catalysis. *Nat. Catal* **2020**, *3*, 401. (c) Mao, R.; Balon, J.; Hu, X. Decarboxylative $C(sp^3)$−O cross-coupling. *Angew. Chem., Int. Ed.* **2018**, *57*, 13624. (d) Chen, Z.; Jiang, Y.; Zhang, L.; Guo, Y.; Ma, D. Oxalic Diamides and *tert*-Butoxide: Two Types of Ligands Enabling Practical Access to Alkyl Aryl Ethers via Cu-Catalyzed Coupling Reaction. *J. Am. Chem. Soc.* **2019**, *141*, 3541. For recent work on Cu-catalyzed $C(sp^2)$−O bond formation, see: (e) Sang, R.; Korkis, S. E.; Su, W.; Ye, F.; Engl, P. S.; Berger, F.; Ritter, T. Site-Selective C−H Oxygenation via Aryl Sulfonium Salts. *Angew. Chem., Int. Ed.* **2019**, *58*, 16161.

(15) For previous work on Fe catalyzed C−O bond formation, see: (a) Xia, N.; Taillefer, M. Copper- or Iron-Catalyzed Arylation of Phenols from respectively Aryl Chlorides and Aryl Iodides. *Chem. - Eur. J.* **2008**, *14*, 6037. (b) Bistri, O.; Correa, A.; Bolm, C. Iron-Catalyzed C−O Cross-Couplings of Phenols with Aryl Iodides. *Angew. Chem., Int. Ed.* **2008**, *47*, 586.

(16) Beletskaya, I. P.; Cheprakov, A. V. Copper in Cross-Coupling Reactions: The Post-Ullmann Chemistry. *Coord. Chem. Rev.* **2004**, *248*, 2337.

(17) For recent reviews on Ni catalysis, see: (a) Tasker, S. Z.; Standley, E. A.; Jamison, T. F. Recent Advances in Homogeneous Nickel Catalysis. *Nature* **2014**, *509*, 299. (b) Standley, E. A.; Tasker, S. Z.; Jensen, K. L.; Jamison, T. F. Nickel Catalysis: Synergy between Method Development and Total Synthesis. *Acc. Chem. Res.* **2015**, *48*, 1503. (c) Diccianni, J. B.; Diao, T. Mechanisms of Nickel-Catalyzed Cross-Coupling Reactions. *Trends in Chemistry* **2019**, *1*, 830. (d) Cavedon, C.; Seeberger, P. H.; Pieber, B. Photochemical Strategies for Carbon−Heteroatom Bond Formation. *Eur. J. Org. Chem.* **2020**, *2020*, 1379. (e) Lavoie, C. M.; Stradiotto, M. Bisphosphines: A Prominent Ancillary Ligand Class for Application in Nickel-catalyzed C−N Cross-coupling. *ACS Catal.* **2018**, *8*, 7228.

(18) (a) Mann, G.; Hartwig, J. F. Nickel- vs Palladium-Catalyzed Synthesis of Protected Phenols from Aryl Halides. *J. Org. Chem.* **1997**, *62*, 5413. For an example using vinyl iodides and $Ni(COD)_2$ without ligand, see: (b) Han, S.-J.; Doi, R.; Stoltz, B. M. Nickel-Catalyzed Intramolecular C−O Bond Formation: Synthesis of Cyclic Enol Ethers. *Angew. Chem., Int. Ed.* **2016**, *55*, 7437.

(19) MacQueen, P. M.; Tassone, J. P.; Diaz, C.; Stradiotto, M. Exploiting Ancillary Ligation To Enable Nickel-Catalyzed C−O Cross Couplings of Aryl Electrophiles with Aliphatic Alcohols. *J. Am. Chem. Soc.* **2018**, *140*, 5023.

(20) (a) Terrett, J. A.; Cuthbertson, J. D.; Shurtleff, V. W.; MacMillan, D. W. C. Switching on Elusive Organometallic Mechanisms with Photoredox Catalysis. *Nature* **2015**, *524*, 330. (b) Cavedon, C.; Madani, A.; Seeberger, P. H.; Pieber, B. Semiheterogeneous Dual Nickel/Photocatalytic (Thio)etherification Using Carbon Nitrides. *Org. Lett.* **2019**, *21*, 5331. (c) Yang, L.; Lu, H.-H.; Lai, C.-H.; Li, G.; Zhang, W.; Cao, R.; Liu, F.; Wang, C.; Xiao, J.; Xue, D. Light-Promoted Nickel Catalysis: Etherification of Aryl Electrophiles with Alcohols Catalyzed by a Ni^{II}-Aryl Complex. *Angew. Chem., Int. Ed.* **2020**, *59*, 12714.

(21) Welin, E. R.; Le, C.; Arias-Rotondo, D. M.; McCusker, J. K.; MacMillan, D. W. C. Photosensitized, Energy Transfer-Mediated Organometallic Catalysis Through Electronically Excited Nickel(II). *Science* **2017**, *355*, 380.

(22) (a) Zhu, B.; Yan, L.-K.; Geng, Y.; Ren, H.; Guan, W.; Su, Z.-M. Ir^{III}/Ni^{II}-Metallaphotoredox Catalysis: the Oxidation State Modulation Mechanism Versus the Radical Mechanism. *Chem. Commun.* **2018**, *54*, 5968. (b) Tian, L.; Till, N. A.; Kudisch, B.; MacMillan, D. W. C.; Scholes, G. D. Transient Absorption Spectroscopy Offers Mechanistic Insights for an Iridium/Nickel-Catalyzed C−O Coupling. *J. Am. Chem. Soc.* **2020**, *142*, 4555. (c) Ma, P.; Wang, S.; Chen, H. Reactivity of Transition-Metal Complexes in Excited States: C−O Bond Coupling Reductive Elimination of a Ni(II) Complex Is Elicited by the Metal-to-Ligand Charge Transfer State. *ACS Catal.* **2020**, *10*, 1.

(23) Zhang, S.-K.; Struwe, J.; Hu, L.; Ackermann, L. Nickela-electrocatalyzed C−H Alkoxylation with Secondary Alcohols: Oxidation-Induced Reductive Elimination at Nickel(III). *Angew. Chem., Int. Ed.* **2020**, *59*, 3178.

(24) Sun, R.; Qin, Y.; Nocera, D. G. General Paradigm in Photoredox Ni-Catalyzed Cross-Coupling Allows for Light-Free Access to Reactivity. *Angew. Chem., Int. Ed.* **2020**, *59*, 9527.

(25) For an example from well-defined Ni^{III} complex, see: Zhou, W.; Schultz, J. W.; Rath, N. P.; Mirica, L. M. Aromatic Methoxylation and Hydroxylation by Organometallic High-Valent Nickel Complexes. *J. Am. Chem. Soc.* **2015**, *137*, 7604.

(26) Smith, S. M.; Planas, O.; Gómez, L.; Rath, N. P.; Ribas, X.; Mirica, L. M. Aerobic C−C and C−O Bond Formation Reactions Mediated by High-Valent Nickel Species. *Chem. Sci.* **2019**, *10*, 10366.

(27) (a) Matsunaga, P. T.; Hillhouse, G. L.; Rheingold, A. L. Oxygen-Atom Transfer from Nitrous Oxide to a Nickel Metallacycle. Synthesis, Structure, and Reactions of [cyclic] (2,2′-bipyridine)Ni-$(OCH_2CH_2CH_2CH_2)$. *J. Am. Chem. Soc.* **1993**, *115*, 2075. (b) Matsunaga, P. T.; Mavropoulos, J. C.; Hillhouse, G. L. Oxygen-Atom Transfer from Nitrous oxide (N═N═O) to Nickel Alkyls. Syntheses and Reactions of Nickel(II) Alkoxides. *Polyhedron* **1995**, *14*, 175. (c) Koo, K.; Hillhouse, G. L.; Rheingold, A. L. Oxygen-Atom Transfer from Nitrous Oxide to an Organonickel(II) Phosphine Complex. Syntheses and Reactions of New Nickel(II) Aryloxides and the Crystal Structure of $(Me_2PCH_2CH_2PMe_2)Ni(0\text{-}o\text{-}C_6H_4CMe_2CH_2)$. *Organometallics* **1995**, *14*, 456. (d) Koo, K.; Hillhouse, G. L. Formation of a Substituted Tetrahydrofuran by Formal [2 + 2 + 1] Coupling of an Oxygen Atom with Two Olefins at a Nickel Center. *Organometallics* **1998**, *17*, 2924.

(28) Desnoyer, A. N.; Bowes, E. G.; Patrick, B. O.; Love, J. A. Synthesis of 2-Nickela(II)oxetanes from Nickel(0) and Epoxides: Structure, Reactivity, and a New Mechanism of Formation. *J. Am. Chem. Soc.* **2015**, *137*, 12748.

https://dx.doi.org/10.1021/jacs.0c07381
J. Am. Chem. Soc. XXXX, XXX, XXX−XXX

(29) (a) Binger, P.; Doyle, M. J.; Krüger, C.; Tsay, Y.-H. Z. Metallacycloalkane, III Darstellung und Charakterisierung von a.a′-Dipyridyl-Nickelacyclopentan /Preparation and Characterisation of a,a′-Bipyridyl-nickelacyclopentane. *Z. Naturforsch., B: J. Chem. Sci.* **1979**, *34B*, 1289. (b) Cámpora, J. Nickel−Carbon σ-Bonded Complexes. *Comprehensive Organometallic Chemistry III* **2007**, *8*, 27−132. (c) Echavarren, A. M.; Castaño, A. M. Oxa-and Azametallacycles of Nickel: Fundamental Aspects and Synthetic Applications. *Adv. Met.-Org. Chem.* **1998**, *6*, 1−47.

(30) Avicel is a powder composed by small particles of cellulose. It is efficient for the removal of Ni black nanoparticles through filtration.

(31) See Supporting Information for more details.

(32) Selectivity issues in the O-insertion step were not considered in the early work from Hillhouse, and preference for the secondary carbon was always obtained. See ref 27b.

(33) (a) Camasso, N. M.; Sanford, M. S. Design, Synthesis, and Carbon-Heteroatom Coupling Reactions of Organometallic Nickel-(IV) Complexes. *Science* **2015**, *347*, 1218. (b) Yu, S.; Dudkina, Y.; Wang, H.; Kholin, K. V.; Kadirov, M. K.; Budnikova, Y. H.; Vicic, D. A. Accessing Perfluoroalkyl Nickel(II), (III), and (IV) Complexes Bearing a Readily attached $[C_4F_8]$ ligand. *Dalton Trans.* **2015**, *44*, 19443.

(34) Moreover, two reductive waves were also observed at −2.1 and −2.71 V vs Fc/Fc^+, corresponding to Ni^{II}/Ni^{I} and Ni^{I}/Ni^{0} couples, respectively. See SI for details.

(35) (a) Luo, J.; Zhang, J. Donor−Acceptor Fluorophores for Visible-Light-Promoted Organic Synthesis: Photoredox/Ni Dual Catalytic $C(sp^3)-C(sp^2)$ Cross-Coupling. *ACS Catal.* **2016**, *6*, 873. (b) Le Vaillant, F.; Garreau, M.; Nicolai, S.; Gryn'ova, G.; Corminboeuf, C.; Waser, J. Fine-Tuned Organic Photoredox Catalysts for Fragmentation-Alkynylation Cascades of Cyclic Oxime Ethers. *Chem. Sci.* **2018**, *9*, 5883.

(36) The reaction was also tested in the original solvent used by Hillhouse (benzene-d_6) with similar results as for CD_2Cl_2. In order to be able to follow the reaction at low temperature, CD_2Cl_2 was preferred due to its low melting point and single peak in NMR.

(37) Kalvet, I.; Guo, Q.; Tizzard, G. J.; Schoenebeck, F. When Weaker Can Be Tougher: The Role of Oxidation State (I) in P- vs N-Ligand-Derived Ni-Catalyzed Trifluoromethylthiolation of Aryl Halides. *ACS Catal.* **2017**, *7*, 2126.

(38) Stanbury, D. M.; Sykes, A. G. *Advances in Inorganic Chemistry*; Academic Press: New York, 1989; Vol. 33; p 69.

(39) (a) Diccianni, J. B.; Hu, C.; Diao, T. Binuclear, High-Valent Nickel Complexes: Ni−Ni Bonds in Aryl−Halogen Bond Formation. *Angew. Chem., Int. Ed.* **2017**, *56*, 3635. (b) Dürr, A. B.; Fisher, H. C.; Kalvet, I.; Truong, K.-N.; Schoenebeck, F. Divergent Reactivity of a Dinuclear (NHC) Nickel(I) Catalyst versus Nickel(0) Enables Chemoselective Trifluoromethylselenolation. *Angew. Chem., Int. Ed.* **2017**, *56*, 13431.

(40) Xu, H.; Diccianni, J. B.; Katigbak, J.; Hu, C.; Zhang, Y.; Diao, T. Bimetallic C−C Bond Forming Reductive Elimination from Nickel. *J. Am. Chem. Soc.* **2016**, *138*, 4779.

(41) (a) Shiren, K.; Ogo, S.; Fujinami, S.; Hayashi, H.; Suzuki, M.; Uehara, A.; Watanabe, Y.; Moro-oka, Y. Synthesis, Structures, and Properties of Bis(μ-oxo)nickel(III) and Bis(μ-superoxo)nickel(II) Complexes: An Unusual Conversion of a $Ni^{III}_2(\mu\text{-}O)_2$ Core into a $Ni^{II}_2(\mu\text{-}OO)_2$ Core by H_2O_2 and Oxygenation of Ligand. *J. Am. Chem. Soc.* **2000**, *122*, 254. (b) Morimoto, Y.; Takagi, Y.; Saito, T.; Ohta, T.; Ogura, T.; Tohnai, N.; Nakano, M.; Itoh, S. A Bis(μ-oxido)dinickel-(III) Complex with a Triplet Ground State. *Angew. Chem., Int. Ed.* **2018**, *57*, 7640. (c) Padamati, S. K.; Angelone, D.; Draksharapu, A.; Primi, G.; Martin, D. J.; Tromp, M.; Swart, M.; Browne, W. R. Transient Formation and Reactivity of a High-Valent Nickel(IV) Oxido Complex. *J. Am. Chem. Soc.* **2017**, *139*, 8718.

(42) (a) Roy, P.; Bour, J. R.; Kampf, J. W.; Sanford, M. S. Catalytically Relevant Intermediates in the Ni-Catalyzed $C(sp^2)-H$ and $C(sp^3)-H$ Functionalization of Aminoquinoline Substrates. *J. Am. Chem. Soc.* **2019**, *141*, 17382. (b) Smith, A. K. In *Comprehensive Organometallic Chemistry II*; Pudephatt, R. J., Ed.; Elsevier, 1995; Vol. 9, Chapter 2.

(43) Stoll, S.; Schweiger, A. EasySpin, a comprehensive software package for spectral simulation and analysis in EPR. *J. Magn. Reson.* **2006**, *178*, 42.

(44) Notice that compounds **2**, **6**, and **7** are volatile, and therefore, calculation of the yield was challenging after filtration of the paramagnetic solids. See ref 31.

(45) (a) Sladek, M. I.; Braun, T.; Neumann, B.; Stammler, H.-G. 3-Fluoropyridyl Nickel Complexes as Useful Tools for the Selective Synthesis of new 2,4,5,6-Tetrafluoropyridines: a Route Complementing the Established Methods to Access Fluorinated Pyridines. *New J. Chem.* **2003**, *27*, 313. (b) Bennett, M. A.; Glewis, M.; Hockless, D. C. R.; Wenger, E. Successive Insertion of Tetrafluoroethylene and CO and of Tetrafluoroethylene and Acetylenes into Aryne−Nickel(0) bonds. *J. Chem. Soc., Dalton Trans.* **1997**, 3105. (c) Coronas, J. M.; Muller, G.; Rocamora, M. Decomposition of [NiRR′L2] Complexes Induced by Bromine or Anodic Oxidation. *J. Organomet. Chem.* **1986**, *301*, 227.

(46) Aihara, Y.; Chatani, N. Nickel-Catalyzed Reaction of C−H Bonds in Amides with I_2: ortho-Iodination via the Cleavage of $C(sp^2)-H$ Bonds and Oxidative Cyclization to β-Lactams via the Cleavage of $C(sp^3)-H$ Bonds. *ACS Catal.* **2016**, *6*, 4323.

(47) (a) Timmons, C.; Chen, D.; Cannon, J. F.; Headley, A. D.; Li, G. New Asymmetric Halo Aldol Reaction Provides a Novel Approach to Biologically Important Chiral Cyclothers and Cycloamines. *Org. Lett.* **2004**, *6*, 2075. For several examples of applications of such cyclization in total syntheses, see: (b) Murata, Y.; Kamino, T.; Aoki, T.; Hosokawa, S.; Kobayashi, S. Highly Efficient Total Synthesis of (+)-Citreoviral. *Angew. Chem., Int. Ed.* **2004**, *43*, 3175. (c) Snyder, S. A.; Brucks, A. P.; Treitler, D. S.; Moga, I. Concise Synthetic Approaches for the Laurencia Family: Formal Total Syntheses of (±)-Laurefucin and (±)-E- and (±)-Z-Pinnatifidenyne. *J. Am. Chem. Soc.* **2012**, *134*, 17714. (d) Yakura, T.; Sato, S.; Yoshimoto, Y. Enantioselective Synthesis of Pachastrissamine (Jaspin B) Using Dirhodium(II)-Catalyzed C−H Amination and Asymmetric Dihydroxylation as Key Steps. *Chem. Pharm. Bull.* **2007**, *55*, 1284.

(48) (a) Brown, R. F.; Van Gulick, N. M. The Geminal Alkyl Effect on the Rates of Ring Closure of Bromobutylamines. *J. Org. Chem.* **1956**, *21*, 1046. (b) Anslyn, E. V.; Dougherty, D. A. *Modern Physical Organic Chemistry*; University Science: Sausalito, CA, 2006.

(49) (a) Nebra, N. High-Valent Ni^{III} and Ni^{IV} Species Relevant to C−C and C−Heteroatom Cross-Coupling Reactions: State of the Art. *Molecules* **2020**, *25*, 1141. (b) Mirica, L. M.; Smith, S. M.; Griego, L. Organometallic Chemistry of High-Valent Ni(III) and Ni(IV) Complexes. In *Nickel Catalysis in Organic Synthesis: Methods and Reactions*; Ogoshi, S., Ed.; Wiley-VCH Verlag GmbH & Co., 2019; pp 223−248.

(50) (a) D'Accriscio, F.; Borja, P.; Saffon-Merceron, N.; Fustier-Boutignon, M.; Mézailles, M.; Nebra, N. C−H Bond Trifluoromethylation of Arenes Enabled by a Robust, High-Valent Nickel(IV) Complex. *Angew. Chem., Int. Ed.* **2017**, *56*, 12898. (b) Meucci, E. A.; Nguyen, S. N.; Camasso, N. M.; Chong, E.; Ariafard, A.; Canty, A.; Sanford, M. S. Nickel(IV)-Catalyzed C−H Trifluoromethylation of (Hetero)arenes. *J. Am. Chem. Soc.* **2019**, *141*, 12872. (c) Bour, J. R.; Camasso, N. M.; Meucci, E. A.; Kampf, J. W.; Canty, A. J.; Sanford, M. S. Carbon−Carbon Bond-Forming Reductive Elimination from Isolated Nickel(III) Complexes. *J. Am. Chem. Soc.* **2016**, *138*, 16105.

(51) For a rare example of $C(sp^3)-CF_3$ bond formation mediated by high-valent copper complexes, see: Liu, S.; Liu, H.; Liu, S.; Lu, Z.; Lu, C.; Leng, X.; Lan, Y.; Shen, Q. $C(sp^3)-CF_3$ Reductive Elimination from a Five-Coordinate Neutral Copper(III) Complex. *J. Am. Chem. Soc.* **2020**, *142*, 9785.

(52) (a) Furuya, T.; Kamlet, A. S.; Ritter, T. Catalysis for Fluorination and Trifluoromethylation. *Nature* **2011**, *473*, 470. (b) Lin, X.; Weng, Z. Transition metal complex assisted Csp^3-F bond formation. *Dalton Trans.* **2015**, *44*, 2021. (c) Chen, Y.-Q.; Singh, S.; Wu, Y.; Wang, Z.; Hao, W.; Verma, P.; Qiao, J. X.; Sunoj, R. B.; Yu, J.-Q. Pd-Catalyzed γ-$C(sp^3)-H$ Fluorination of Free Amines.

https://dx.doi.org/10.1021/jacs.0c07381
J. Am. Chem. Soc. XXXX, XXX, XXX−XXX

J. Am. Chem. Soc. **2020**, *142*, 9966. (d) Racowski, J. M.; Gary, J. B.; Sanford, M. S. Carbon(sp^3)−Fluorine Bond-Forming Reductive Elimination from Palladium(IV) Complexes. *Angew. Chem., Int. Ed.* **2012**, *51*, 3414. (e) Hull, K. L.; Anani, W. Q.; Sanford, M. S. Palladium-Catalyzed Fluorination of Carbon-Hydrogen Bonds. *J. Am. Chem. Soc.* **2006**, *128*, 7134. (f) Mankad, N. P.; Toste, F. D. C(sp^3)−F Reductive Elimination from Alkyl Gold(III) Fluoride Complexes. *Chem. Sci.* **2012**, *3*, 72.

(53) (a) Tramšek, M.; Žemva, B. Synthesis, Properties and Chemistry of Xenon(II) Fluoride. *Acta Chim. Slov.* **2006**, *53*, 105. (b) Planas, O.; Wang, F.; Leutzsch, M.; Cornella, J. Fluorination of Arylboronic Esters Enabled by Bismuth Redox Catalysis. *Science* **2020**, *367*, 313. (c) Ball, N. D.; Sanford, M. S. Synthesis and Reactivity of a Mono-σ-Aryl Palladium (IV) Fluoride Complex. *J. Am. Chem. Soc.* **2009**, *131*, 3796.

(54) (a) Rozatian, N.; Ashworth, I. W.; Sandford, G.; Hodgson, D. R. W. *Chem. Sci.* **2018**, *9*, 8692. (b) Lal, G. S.; Pez, G. P.; Syvret, R. G. Electrophilic Fluorinating Agents. *Chem. Rev.* **1996**, *96*, 1737.

(55) Saito, T.; Uchida, Y.; Misono, A.; Yamamoto, A.; Morifuji, K.; Ikeda, S. Diethyldipyridylnickel. Preparation, Characterization, and Reactions. *J. Am. Chem. Soc.* **1966**, *88*, 5198.

(56) (a) Bour, J. R.; Camasso, N. M.; Sanford, M. S. Oxidation of Ni(II) to Ni(IV) with Aryl Electrophiles Enables Ni-Mediated Aryl−CF_3 Coupling. *J. Am. Chem. Soc.* **2015**, *137*, 8034. (b) Meucci, E. A.; Ariafard, A.; Canty, A. J.; Kampf, J. W.; Sanford, M. S. Aryl−Fluoride Bond-Forming Reductive Elimination from Nickel(IV) Centers. *J. Am. Chem. Soc.* **2019**, *141*, 13261. (c) Bour, J. R.; Ferguson, D. M.; McClain, E. J.; Kampf, J. W.; Sanford, M. S. Connecting Organometallic Ni(III) and Ni(IV): Reactions of Carbon-Centered Radicals with High-Valent Organonickel Complexes. *J. Am. Chem. Soc.* **2019**, *141*, 8914. (d) Meucci, E. A.; Camasso, N. M.; Sanford, M. S. An Organometalllic Ni^{IV} Complex That Participates in Competing Transmetalation and C(sp^2)−O Bond-Forming Reductive Elimination Reactions. *Organometallics* **2017**, *36*, 247. (e) See also refs 33a , 49, 50b, and 50c.

(57) It is important to note that fitting of multifrequency EPR experiments on the same compound should certainly enhance the reliability of the obtained parameters. Such multifrequency experiments could probably provide insights into the expected and currently not observed HFI coupling for Ni−F and its magnitude.

(58) Detection of m/z for ***int-II*** and ***int-IV*** from the reaction mixture can also be attributed to fragmentation of a putative dimer during analysis. In addition, a m/z corresponding to dimeric Ni^{III}−Ni^{III} corresponding to the defluorinated ***int-I*** could also be observed. See Supporting Information for details.

(59) For Ni^{III}-F complexes, see: (a) Mondal, P.; Lovisari, M.; Twamley, B.; McDonald, A. R. Fast Hydrocarbon Oxidation by a High-Valent Nickel−Fluoride Complex. *Angew. Chem., Int. Ed.* **2020**, *59*, 13044. (b) Lee, H.; Börgel, J.; Ritter, T. Carbon−Fluorine Reductive Elimination from Nickel(III) Complexes. *Angew. Chem., Int. Ed.* **2017**, *56*, 6966. (c) Zhou, W.; Zheng, S.; Schultz, J. W.; Rath, N. P.; Mirica, L. M. Aromatic Cyanoalkylation through Double C−H Activation Mediated by Ni^{III}. *J. Am. Chem. Soc.* **2016**, *138*, 5777. (d) See also ref 50a.

(60) For Ni^{IV}−F complexes, see: (a) Roberts, C. C.; Chong, E.; Kampf, J. W.; Canty, A. J.; Ariafard, A.; Sanford, M. S. Nickel(II/IV) Manifold Enables Room-Temperature C(sp3)−H Functionalization. *J. Am. Chem. Soc.* **2019**, *141*, 19513. (b) Chong, E.; Kampf, J. W.; Ariafard, A.; Canty, A. J.; Sanford, M. S. Oxidatively Induced C−H Activation at High Valent Nickel. *J. Am. Chem. Soc.* **2017**, *139*, 6058. (c) Kosobokov, M. D.; Sandleben, A.; Vogt, N.; Klein, A.; Vicic, D. A. Nitrogen−Nitrogen Bond Formation via a Substrate-Bound Anion at a Mononuclear Nickel Platform. *Organometallics* **2018**, *37*, 521. (d) See also refs 50a and 56b.

(61) (a) Wolf, W. J.; Winston, M. S.; Toste, F. D. Exceptionally Fast Carbon−Carbon Bond Reductive Elimination from Gold(III). *Nat. Chem.* **2014**, *6*, 159. (b) Powers, D. C.; Benitez, D.; Tkatchouk, E.; Goddard, W. A., III; Ritter, T. Bimetallic Reductive Elimination from Dinuclear Pd(III) Complexes. *J. Am. Chem. Soc.* **2010**, *132*, 14092.

https://dx.doi.org/10.1021/jacs.0c07381
J. Am. Chem. Soc. XXXX, XXX, XXX−XXX